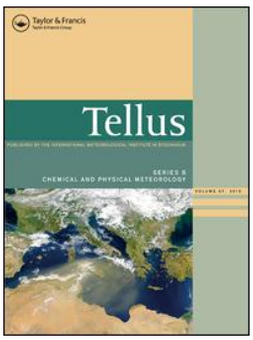

Tellus B: Chemical and Physical Meteorology

ISSN: (Print) 1600-0889 (Online) Journal homepage: http://www.tandfonline.com/loi/zelb20

Structure, variability and persistence of the submicrometre marine aerosol

Jost Heintzenberg, Wolfram Birmili, Alfred Wiedensohler, Andreas Nowak & Thomas Tuch

To cite this article: Jost Heintzenberg, Wolfram Birmili, Alfred Wiedensohler, Andreas Nowak & Thomas Tuch (2004) Structure, variability and persistence of the submicrometre marine aerosol, Tellus B: Chemical and Physical Meteorology, 56:4, 357-367, DOI: 10.3402/tellusb.v56i4.16450

To link to this article: https://doi.org/10.3402/tellusb.v56i4.16450

Published online: 18 Jan 2017.

Tellus (2004), 56B, 357–367
Printed in UK. All rights reserved

TELLUS

Structure, variability and persistence of the submicrometre marine aerosol

By JOST HEINTZENBERG*, WOLFRAM BIRMILI, ALFRED WIEDENSOHLER, ANDREAS NOWAK and THOMAS TUCH, *Leibniz-Institute for Tropospheric Research, Permoserstr. 15, 04318 Leipzig, Germany*

(Manuscript received 3 February 2004; in final form 29 March 2004)

ABSTRACT

Submicrometre dry number size distributions from four marine and one continental aerosol experiment were evaluated jointly in the present study. In the marine experiments only data with back trajectories of at least 120 h without land contact were used to minimize continental contamination. Log-normal functions were fitted to the size distributions. Basic statistics of the marine aerosol indicate a closed character of the size distribution at the lower size limit as opposed to an open character for corresponding continental data. Together with the infrequent occurrences of marine particles below 20 nm this finding supports hypotheses and model results suggesting low probabilities of homogeneous nucleation in the marine boundary layer. The variability of submicrometre marine number concentrations was parametrized with a bimodal log-normal function that quantifies the probability of finding different number concentrations about a given median value. Together with a four-modal log-normal approximation of the submicrometre marine size distribution itself, this model allows a statistical representation of the marine aerosol that facilitates comparison of experiments and validation of aerosol models. Autocorrelation at the one fixed marine site with a minimum of interruptions in times-series revealed a strong size dependency of persistence in particle number concentration with the shortest persistence at the smallest sizes. Interestingly, in the marine aerosol (at Cape Grim) persistence exhibits a size dependency that largely matches the modes in d_{g0}, i.e. near the most frequent geometric mean diameters number concentrations are most persistent. Over the continent, persistence of particle numbers is strongly constrained by diurnal meteorological processes and aerosol dynamics. Thus, no strong modal structure appears in the size-dependent persistence at Melpitz. As with the aerosol variability, marine aerosol processes in models of aerosol dynamics can be tested with these findings.

1. Introduction

The International Global Atmospheric Chemistry Program (IGAC) formulated a number of regional aerosol characterization experiments (ACE) to improve our understanding of the marine aerosol, its formation processes and its effects. Consequently, from 1995 to 2001 a series of large marine aerosol experiments took place, which, together with the Indian Ocean Experiment (INDOEX, 1998–2000), greatly enhanced the marine aerosol database. These data stimulated several reviews, syntheses and compilations concerning the marine aerosol that focused on different physical and chemical aspects. The largely retrospective review of Heintzenberg et al. (2000) had a geographical focus and synthesized the available physical and chemical aerosol data as average meridional distributions. This review also reported modal functional approximations in terms of log-normal size distributions as had been done previously for the Arctic aerosol by Covert et al. (1996) and later for other individual marine aerosol experiments by Bates et al. (2000, 2002). The latter also provided typical air mass-related number size distributions but did not include ultrafine particles (UFPs) below 20 nm.

Geographical, meteorological and modal interpretations of the measured size distributions provide useful data for the validation of aerosol results derived with large-scale chemical transport models (CTMs) and global climate models (GCMs). Because of inherent model limitations the first such validation exercise utilized monthly means of point measurements (Langner et al., 1993). With increasing spatiotemporal resolution of the CTMs, higher-resolution aerosol data could be utilized to assess the model performance. Total sulfate with 24-h time resolution from many stations were employed by Benkovitz et al. (1994) and Benkovitz and Schwartz (1997) to test the ability of their models to simulate the magnitudes and temporal development of observed sulfate concentrations. Meanwhile, CTMs and GCMs have started to incorporate simple aerosol dynamical processes, simulating size-dependent aerosol information (Rasch et al., 2000; Jacobson, 2001; Wilson et al., 2001). The

*Corresponding author.
e-mail: jost@tropos.de

extreme non-linearity of aerosol dynamics coupled with the complexity of atmospheric dynamics and radiative transfer requires a detailed validation of the related models with size-dependent high-resolution aerosol data that reaches far beyond average, typical or air mass-related size distributions. Complete particle size distributions can be recorded with time resolutions of the order of 10 min. The numerical simulation of such aerosol data will remain for quite some time beyond the range of modelling because of incomplete initial atmospheric fields and coarse scales of the simulated processes. For the wrong reasons the model may even reproduce individual aerosol events correctly. For this reason, model validations in meteorology rely on statistical verifications based on large databases and similar approaches are warranted with CTMs.

The present study takes a statistical synthesizing approach based on a large number of dry size distributions of marine aerosol particles taken in 1995, 1997, 1999 and 2001 near the sea surface over the Atlantic, Pacific, Indian and Southern oceans. For the present study only data with at least 120 h traveltime (according to trajectories) from the nearest land have been included. The structure of the submicrometre size distribution is analysed with log-normal approximations that reduce the number of parameters from the measured >40 to 12. Size-dependent and integral variability of number concentrations and persistence of the submicrometre number size distribution are discussed with the unfitted size distributions. Most of the data in the present analysis have not been reported previously. Instead, similar data taken in parallel on different platforms of the same experiment have been discussed in the literature. For the 1999 experiment, no UFP data have been published before.

With this new approach a number of questions will be addressed: What is the probability distribution of different particle sizes in the marine boundary layer (MBL)? What is the probability of occurrence of UFP? What is the variability of submicrometre number concentration? How does this variability change depending on particle size? What is the persistence of the size distribution as a function of particle size? How do frequencies of occurrence relate to the modal structure of the number size distribution? After an introduction to the database and a description of the data processing size-dependent probability distribution functions (PDFs) will be discussed in the light of the questions posed above. In order to demonstrate the uniqueness of the marine aerosol size distribution we contrast our marine distribution with those for a data set from a site in Central Europe, taken with the same instrumentation.

2. Database

The database stems from measurements with twin differential mobility particle spectrometers (TDMPS) taken by the Institute for Tropospheric Research (IfT) during four international aerosol experiments. Instrumental details can be found in Birmili and Wiedensohler (1997). During IGAC's first aerosol characterization experiment (ACE-1) (Bates et al., 1998a) a TDMPS was stationed at the Australian baseline station (Cape Grim, www.bom.gov.au). The instrument scanned 96 equal logarithmic steps from 3.1 to 650 nm dry diameter with a time resolution of 10 min. A first report of TDMPS data from this experiment can be found in Covert et al. (1998). Ship-borne measurements from the same experiment with a similar measurement system have been classified by air mass and particle modes in Bates et al. (1998b).

During the ACE-2 experiment (Raes et al., 2000) the same system was operated at the coastal station Sagres, Portugal as part of an aerosol closure experiment (Russell and Heintzenberg, 2000). Forty equal logarithmic steps from 3.1 to 790 nm dry diameter were scanned with a time resolution of 15 min. Again, ship-borne measurements from the same experiment with a similar measurement system have been classified by air mass and particle modes in Bates et al. (2000). Within the framework of ACE-2 other groups in land- and ship-borne experiments operated additional aerosol spectrometers. Their data were not included in the present study because of significant differences in hardware and evaluation procedures.

A ship-borne TDMPS system of the same design was operated during the AEROSOL99/INDOEX cruise of the R/V *Ronald H. Brown* (Bates et al., 2002). The TDMPS scanned 41 equal logarithmic steps from 3 to 900 nm dry diameter with a time resolution of 17 min. The cruise started in Norfolk, Virginia, went on a nearly straight great-circle course to Cape Town, South Africa, from there to the INDOEX operational area and ended at Male, Maldives. The INDOEX area covered the southern and northern Indian Ocean, the Arabian Sea, and the Bay of Bengal.

Finally the TDMPS data taken on R/V *Ronald H. Brown* during the ACE-Asia experiment were included in the database. Details of this experiment can be found at http://saga.pmel.noaa.gov/aceasia/. During the measurements the ship moved from Hawaii to the ACE-Asia operational region between China, Korea and Japan, ending the cruise in Yokohama, Japan. The scan settings were the same as in the 1999 experiment.

In order to demonstrate the uniqueness of the uncontaminated marine Aerosol, its variability and persistence is contrasted with a continental data set taken with the same instrumentation at the central European research station at Melpitz, Germany in summer 1996. There, 48 logarithmically equal steps were scanned between 3 and 614 nm. These data have been discussed considering aspects different from the present study in Birmili and Wiedensohler (2000) and Birmili et al. (2001). Beyond the original quality control no additional data processing was applied to this data set. Table 1 summarizes the characteristics of each experiment.

3. Data processing

The concentration at a given size interval of an aerosol number size distribution derived with particle counters is determined by,

Table 1. Characteristics of the four marine aerosol experiments and the continental reference experiment of the present study. % > 120 h is the percentage of data with more than 120 h traveltime from the nearest land contact. N_{fit} is the number of distributions fitted with ≥ 2 log-normal functions

Experiment	Location	Time period	No of records	% > 120 h	N_{fit}
ACE-1	Cape Grim (40.82°S, 144.73°E)	17 Nov.–14 Dec. 1995	1686	81	1354
ACE-2	Sagres, Portugal (36.98°N, 8.95°W)	15 Jun.–24 Jul. 1997	2474	23	595
Aerosols99/INDOEX	N/S Atlantic, Indian Ocean	15 Jan.–30 Mar. 1999	4311	80	2713
ACE-Asia	Pacific, Yellow Sea, Sea of Japan	16 Mar.–20 Apr. 2001	1966	23	266
Melpitz 1996	Melpitz, Germany (51.5°N, 12.9°E)	26 Mar.–30 Sept. 1996	16 044	0	9183

among other things, Poisson counting statistics. In the present data set this uncertainty becomes large at both ends of the range of particle diameters analysed. Below a particle diameter of 20 nm the data are based on a TSI-3025 ultrafine particle counter (TSI Inc, St Paul MN, USA), which has a low-volume flow of sample air with ensuing high counting uncertainties. Above a particle diameter of 20 nm, the use of a TSI-3020 with a 16.7 times higher sample flow greatly reduced counting uncertainties. However, close to the upper limit of the diameter range analysed number concentrations of atmospheric aerosol particles in general become low, which again raises counting uncertainties, even at the higher flows. For the present study Poisson counting statistics were checked for each recording. Only concentrations with counting uncertainties of 100% or less were accepted for subsequent data processing and analyses.

Before synthesizing the measured number size distributions they were interpolated to a common grid of particle sizes that encompassed as many of the diameters of the four individual marine experiments as possible. This grid comprises 42 diameters reaching from 3.7 to 613 nm with an average spacing of 13% in between. The logarithms of the number concentrations were interpolated on this size grid.

Latitude, longitude and time of the measuring platform were known for every TDMPS measurement in the four marine experiments. For the ship platforms the position data of the vessel was linearly interpolated for the aerosol recording times in between the available position records. With this information the origin of the measured aerosol was estimated with 5-day back trajectories calculated using the HYSPLIT 4 model. A description of HYSPLIT can be found on http://www.arl.noaa.gov/ready/sec/hysplit4.html. For 1997 and later the model runs were made using Global FNL meteorological fields. For 1995 reanalysis data were used. Vertical motions were calculated from the vertical velocity (omega) field. Trajectories were calculated to all sampling sites at 6-h intervals for trajectories arriving at the actual location at 500 m. This height is a compromise between the requirement of (1) an arrival height that corresponds to the elevations of the different sampling points (between 12 and 100 m above sea level), (2) is representative for the MBL and (3) does not cause the calculated trajectories to hit the lower boundary of the meteorological fields. For Cape Grim Tully and Downey (2003) found the best correlation between measured radon concentrations and trajectories for an arrival height of 500 m. The trajectories for 1999 and 2001 have been taken from http://saga.pmel.noaa.gov/indoex/traject/index.html and http://saga.pmel.noaa.gov/aceasia/rhb_data/traject/, respectively. With these trajectories traveltimes in hours from the nearest land contact were estimated and interpolated linearly for the TDMPS data positions in between the 6-h trajectory intervals. For travel times beyond the range of the calculated trajectories (120 h and longer) the aerosol data were flagged as low-contamination marine.

Multiple log-normal curves were fitted to the experimental particle size distributions using a moment-preserving least-squares fitting algorithm (Birmili, 2001; Birmili et al., 2001). During this procedure, not only were the number size distributions fitted but also, simultaneously, the distributions of the moments +2 and +4. This improved the numerical stability (convergence) of the least-squares algorithm and also ensured that the log-normal modes represented the upper tail of the size distribution (where concentrations are low) with the same accuracy as near the centre of the distribution. Optimization of the curve parameters of an experimental distribution always started with a guess of four log-normal modes, evenly distributed across the diameter range of the distribution to be analysed. This set of 12 initial guess parameters, (F_{m0}, d_{g0}, σ_g for each of the four modes), was improved during a cycle of 30 individual runs ("steps") of the least-squares algorithm. Importantly, each of the 30 individual fitting steps allowed the variation of a subset of the 12 log-normal parameters only. In particular, the three parameters of a single mode (F_{m0}, d_{g0}, σ_g) were optimized during one single run, or the eight parameters concerning amplitude and geometric mean diameter (F_{m0}, d_{g0}) of all modes. By rotating the parameters to be fitted among all possible modes, all 12 curve parameters were allowed to gradually improve several times. This optimization strategy, optimizing in each step only a subset of the 12 parameters, treats the initial guess parameters in a more conservative manner, which improved the physical meaningfulness of the results; unrealistic parameter values like $\sigma_g > 3$, or pairs of d_{g0} very close to each other, which usually occur when fitting all log-normal modal parameters simultaneously, were avoided.

Once the 12 log-normal parameters had been successively optimized in a cycle of 30 steps, the set of parameters was checked for potentially redundant modes. The redundancy of a mode was defined when its diameter d_{g0} was in a ratio smaller than 1.8 (Melpitz: 1.6) with the d_{g0} of a neighbouring mode. In that case, the number of modes was reduced to three, and the fit procedure repeated from the beginning. Similarly, the number was further reduced to two if the redundancy of a mode was determined from the results of the three-modal fit. In summary, multiple log-normal fits were obtained for the experimental distributions having two, three or four modes, depending on each individual distribution. Strictly speaking, the choice of d_{g0} ratios is arbitrary. The values for marine and continental conditions were determined after plotting time-series of modal parameters retrieved with different ratios. Those time-series with a minimum of jumps between the number of modes were considered the most physical representations of the atmospheric aerosol, and the related ratios were employed thereafter.

To further improve the fitting results, the fits were rerun on the basis of an additional cycle of 30 fitting steps. This time, additional initial guess parameters were taken from a database of successful fits that had been obtained from the first evaluation step described above. For each distribution to be fitted, the log-normal parameters of the four most similar (and successfully fitted) distributions available were offered as initial guesses, two of which were prescribed to be three-modal, and two of which were prescribed to be four-modal. If a fit using any of those additional initial guesses was found to improve the present fit, the respective fitting parameters were used as final values instead of those obtained in the first evaluation round. By this procedure, typically 30–50% of the log-normal fits were improved.

Once all 12 log-normal parameters had been successively optimized, the set of parameters was checked for potentially redundant modes. The redundancy of a mode was defined when its diameter d_{g0} was in a ratio smaller than 1.8 (Melpitz: 1.6) with the d_{g0} of a neighbouring mode. In that case, the number of modes was reduced to three, and the fit procedure repeated from the beginning. Similarly, the number was further reduced to two if the redundancy of a mode was determined from the results of the three-modal fit. In summary, multiple log-normal fits were obtained for the experimental distributions having two, three or four modes.

For the present dataset from four marine experiments the average relative deviation between measured and fitted data was 0.080 with a standard deviation of 0.047.

4. Results

The conventional evaluation of functional approximations such as log-normal fits of individual particle size distributions entails the following statistics. The fit in Section 4.1 aggregates the size distributions over timescales of the order of 15 min or air volumes of the order of 10 l before incorporating them in the overall statistics of an experiment, which comprises timescales of weeks or sampled volumes of the order of 50 m^3. If the variability of the size distribution would only be caused by random dilutions of the whole submicrometre particle population then the overall statistics of number concentrations would yield the same modes in particle size as the procedures discussed in Section 4.1. This issue is pursued in Section 4.2 with a variability analysis based on non-aggregated size-dependent number concentrations of the complete experiments. Finally, the size-dependent persistence of the submicrometre size distribution will be analysed in terms of autocorrelations in Section 4.3. With the exception of Section 4.3 all analyses are based on data with at least 120 h of traveltime since the latest land contact of back trajectories.

4.1. Structure of the submicrometre size distributions

For the most basic exploratory structural analysis size-dependent 5th, 50th and 95th percentiles of number concentrations calculated over all experiments are plotted in Fig. 1 in comparison with respective continental results. Three main differences appear between marine and continental size distributions:

(1) Marine number percentiles are about one order of magnitude lower than continental ones.

(2) More structure is visible in the marine size distributions, indicating several relative maxima or modes that will be explored further.

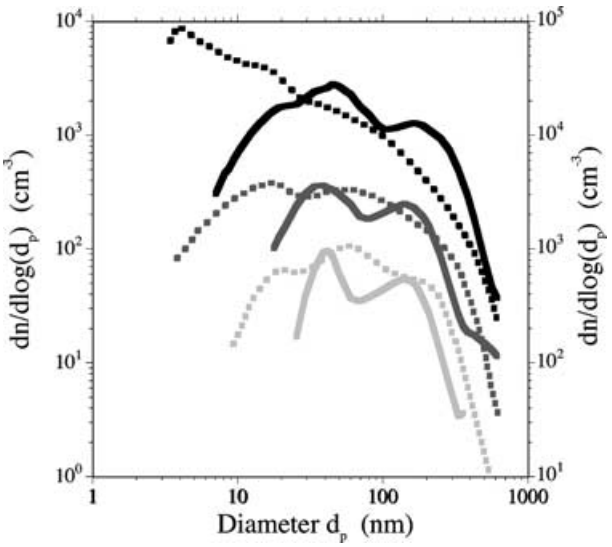

Fig 1. Size-dependent 5% (light grey), 50% (dark grey) and 95% (black) percentiles of number concentrations calculated for all marine experiments detailed in Table 1 and traveltimes *ge*120 h since the latest land contact. For comparison respective results are plotted for data taken at Melpitz, Germany 1996. Marine results are displayed on the left hand scale whereas the continental data are shown on the right hand scale.

(3) Whereas the marine size distributions appear closed near the nominal lower size limit of the atmospheric aerosol, continental ones remain open, at least when considering the 95th percentile.

The latter result supports important speculations that have been discussed in many studies relating to the formation of the marine aerosol. The open continental size distributions suggest frequent occurrences of homogeneous particle nucleation with subsequent condensational particle growth into the measurable size range. In the MBL this process appears to be much less frequent. Closed marine size distributions indicate that either particle nucleation occurred some time ago, most likely outside the MBL in the free troposphere with subsequent downward mixing (Raes, 1995; Shaw et al., 1998), or that other (heterogeneous) processes, as suggested by Leck and Bigg (1999), controlled new particle formation in the MBL that would require primary particle sizes within the measurable size range.

Log-normal fits of size distributions are a valuable tool for structural analyses because they emphasize the appearance of relative maxima while reducing the number of distribution parameters. As a starting point, the relative frequency of occurrence of geometric mean diameters (PDFd_{g0}) in all marine experiments is plotted in Fig. 2. As expected from numerous earlier analyses of marine and continental aerosol size distributions (e.g. Covert et al., 1996; Mäkelä et al., 2000; Birmili et al., 2001; Tunved et al., 2003), PDFd_{g0} showed strong frequency maxima in certain diameter ranges. The smallest and largest mode suffered from specific limitations. The probability of occurrence of ultrafine particles generally was low (*cf.* Section 4.2) and the data of the ultrafine CPC were severely constrained by Poisson statistics. The fourth (sea-salt) mode, on the other hand, reaches beyond the upper end of instrumental size range. Also, here, Poisson statistics limited the information content of the data. Thus, the fitting results of this mode will not be representative for the whole sea-salt size distribution.

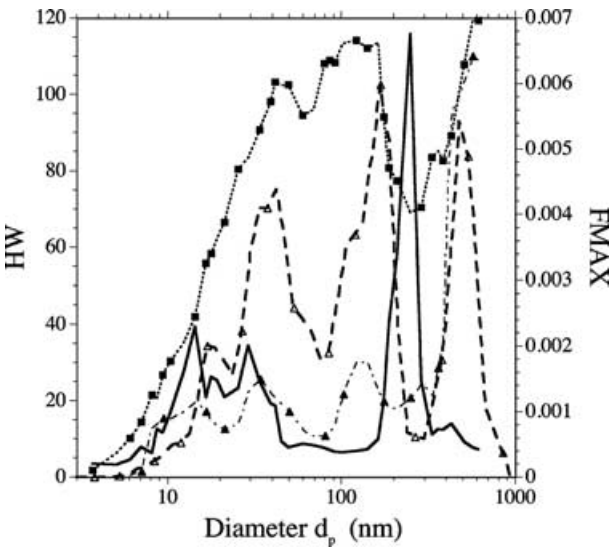

Fig 2. Relative size-dependent frequencies of occurrence of geometric mean diameters (PDF$d_{g0}(d_p)$) (dashed line with open triangles, right-hand scale) in all marine experiments detailed in Table 1 and traveltimes $\geq$ 120 h since the latest land contact. Size-dependent maximum in frequency of occurrence FMAX(d_p) (dotted line with black squares) of number concentrations between 1 and 10 000 cm^{-3}, relative half width (HW) of PDF$_N(d_p)$ (black line) and size-dependent persistence $T_{0.5}(d_p)$ (dash-dotted line with black triangles, left-hand scale) in experiment ACE-1; see Section 4 for details.

Statistics of the log-normal fit parameters of the four experiments are collected in Table 2. The number size distributions with median values of log-normal parameters illustrated in Fig. 3 indicate the similarities and differences between the four experiments. Only the median distributions of ACE-2 and ACE-Asia exhibit UFP modes. The other experiments (and grand average (GA) statistics) only show UFP modes in the 95th percentile rows of Table 2. In GA statistics (not shown in Table 2) the percentile level has to be raised to 78% before an UFP mode appears. Modes two and three and their respective range of values are comparable to Aitken and accumulation modes as given in the marine review of Heintzenberg et al. (2000). The fourth (sea-salt) mode exhibits similar geometric mean diameters in all four experiments.

The fact that the marine number size distributions appear closed at the lower size end (*cf.* Fig. 1) and that the modal diameters exhibited rather similar values between 15 and 20 nm in all experiments suggests (1) that the related nucleation events occurred on the order of hours ago (Kulmala et al., 2004) and (2) that these events proceeded in similar ways. One may speculate that these nucleation events did not take place near the sea surface but possibly in the free troposphere as suggested by hypotheses and modelling results of Raes (1995) and Shaw et al. (1998) and by experimental findings (e.g. Clarke et al., 1996).

Total concentrations in the four modes vary considerably between the experiments. In all modes except for the sea-salt mode the highest number concentrations were found over the polluted North Atlantic. At Cape Grim and in ACE-Asia the highest sea-salt concentrations were found. The widths of the log-normal modes are rather similar and do not differ strongly between the experiments. In general, geometric standard deviations are somewhat smaller than corresponding values given in Heintzenberg et al. (2000). A more comprehensive data set taken partly with higher size resolution is suspected to have caused the differences.

4.2. Variability of the marine number size distribution

From the spread of the percentiles in Fig. 1 a first idea of the variability of size-dependent marine number concentrations can be gleaned. For a more detailed way of analysing this variability, PDFs of the number concentrations $N(d_p) = \mathrm{d}N(d_p)/\mathrm{d}\log(d_p)$ were constructed by classifying the number size distributions

Table 2. Statistics of log-normal fit parameters of the marine submicrometre number size distribution of aerosol particles (*cf.* Table 1 for details of the experiments): GA, grand average; %, percentile of the population of log-normal parameters; d_{gi}, geometric mean diameters; N_i, total number (cm^{-3}); σ_{gi}, geometric standard deviations; $i = 1$, ultrafine mode; $i = 2$, Aitken mode; $i = 3$, accumulation mode; $i = 4$, coarse (sea-salt) mode

Experiment	%	d_{g1}	d_{g2}	d_{g3}	d_{g4}	N_1	N_2	N_3	N_4	σ_{g1}	σ_{g2}	σ_{g3}	σ_{g4}
ACE-1	5	11	20	84	331	0	36	11	3	1.1	1.3	1.3	1.3
ACE-1	50	16	33	120	454	0	266	89	10	1.3	1.4	1.4	1.5
ACE-1	95	19	53	174	577	532	394	171	26	1.5	1.7	1.7	2.0
ACE-2	5	9	29	99	252	0	177	0	0	1.1	1.3	1.3	1.1
ACE-2	50	19	46	161	495	248	1089	186	4	1.4	1.5	1.4	1.3
ACE-2	95	26	74	203	658	1866	2651	510	369	1.7	1.7	1.6	1.9
Aerosols99/INDOEX	5	16	30	97	260	0	7	16	0	1.1	1.3	1.3	1.2
Aerosols99/INDOEX	50	22	46	157	527	0	119	93	2	1.2	1.4	1.4	1.4
Aerosols99/INDOEX	95	27	81	208	772	45	381	527	19	1.5	1.6	1.6	2.0
ACE-Asia	5	11	32	104	264	0	0	2	1	1.2	1.3	1.3	1.2
ACE-Asia	50	17	47	148	523	33	52	80	10	1.3	1.4	1.4	1.4
ACE-Asia	95	23	79	193	721	495	270	593	52	1.4	1.8	1.6	2.0
GA	5	9	29	95	274	0	0	0	0	1.1	1.3	1.3	1.2
GA	50	18	43	149	487	0	146	98	4	1.3	1.4	1.4	1.4
GA	95	26	81	205	718	640	1275	467	26	1.6	1.7	1.6	2.0

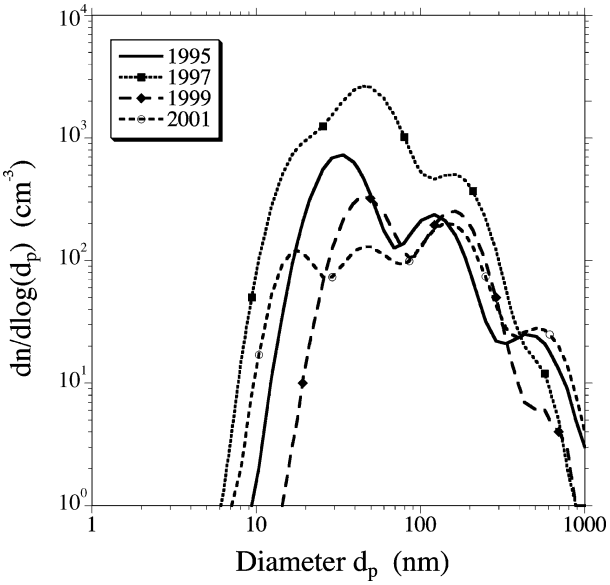

Fig 3. Multimodal log-normal approximations of the number size distributions of the four marine experiments listed in Table 1 constructed with the median values of their respective lognormal parameters (*cf.* Table 2).

of the four marine aerosol experiments in 20 equal logarithmically spaced concentration bins between one and 10 000 cm^{-3}. By dividing the number of cases in each concentration bin by the total number of classified concentrations the probability of $N(d_p)$ occurring within each concentration bin was calculated ($PDF_N(d_p)$). Figure 4 gives an overview of the calculated number PDFs taken over all four experiments. The frequencies of occurrence of different concentrations vary strongly with particle size. Distinct local frequency maxima and minima show up in Fig. 4, which must be related to the controlling aerosol dynamic processes, e.g. a narrow frequency maximum being an indicator of a rather stable aerosol. Two characteristic parameters of $PDF_N(d_p)$ will be discussed for the four experiments: $FMAX(d_p)$ represents the most frequent size-dependent number concentration; $HW(d_p)$ is the ratio of the 75th over the 25th percentile of the number PDF.

Figure 2 shows average results of $FMAX(d_p)$, and $HW(d_p)$ of the four marine experiments. $FMAX(d_p)$ shows two main maxima in the range 40–200 nm, indicating sizes with most stable number concentrations. These maxima roughly coincide with the maxima of $PDFd_{g0}$ in modes two and three. Thus, at the most frequent modal diameters the range of possible number concentrations in the marine aerosol is rather narrow.

As a direct consequence of a probability distribution function, the Half-width of $PDF_N(d_p)$ is generally low in size regions with high values of $FMAX(d_p)$ with an increase towards UFP and a strong maximum above 100 nm. The constraint of the data at the lower size end due to instrumental limitations (Poisson error, *cf.* Section 3) is emphasized. It limits the detectable range of concentrations, which is expected to widen with decreasing UFP size if nucleation events of varying age were recorded. Above UFP sizes $HW(d_p)$, increases from values of between five and ten near the peaks of $PDF_N(d_p)$ to a value greater than 100 near 250 nm. We interpret this peculiar point in the marine number size distribution as the break point between the tail of the sea-salt mode and the gas phase and cloud-derived accumulation mode.

UFPs occurred infrequently in the four marine experiments of the present study, which can be seen from the statistics in

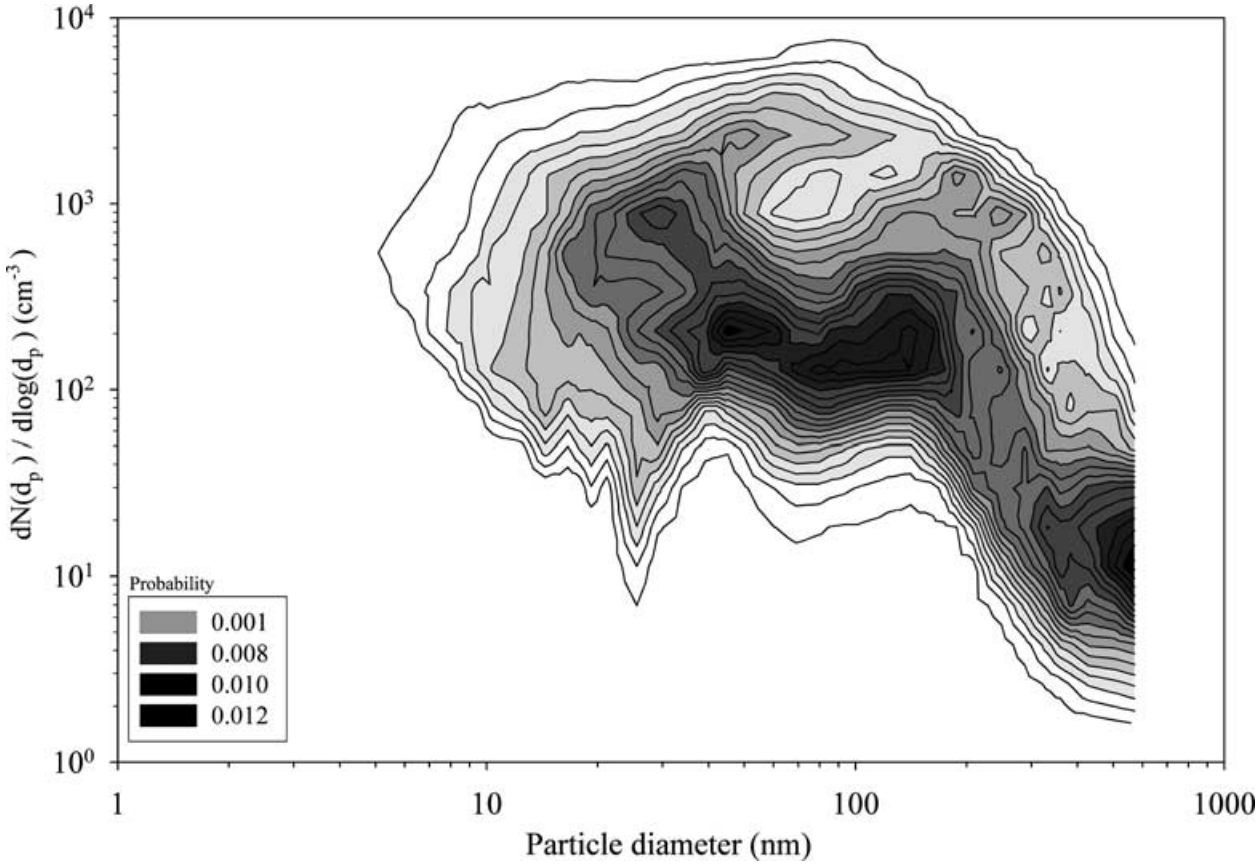

Fig 4. Probability distribution of size-dependent number concentrations ($PDF_N(d_p)$) between 1 and 10 000 cm^{-3} of all four marine experiments listed in Table 1.

Table 2. Cumulative probabilities of occurrences have been calculated from the $PDF_N(d_p)$ of the data from all experiments. In the uncontaminated MBL, particles below 10 (20) nm diameter occur in only 3 (14)% of all recordings. The corresponding probabilities in the continental boundary layer are much higher: 17% below 10 nm and 30% below 20 nm.

The average variability of the uncontaminated submicrometre marine aerosol in the four marine experiments was quantified after normalizing $N(d_p)$ with the respective median concentrations. These normalized concentrations were classified in 20 equal logarithmically spaced concentration bins n between 1% and 100 times the respective median concentrations. The resulting relative frequencies $f(n)$ of occurrence are plotted in Fig. 5 as averages over all particle sizes taken over all four experiments. For comparison the corresponding average variability of the continental data from Melpitz, Germany is shown. The upper wing of the continental distribution is somewhat wider, extending to larger concentrations, relative to the medians, as compared with the marine distributions.

Often the frequency of pollutant concentrations appears to be approximately log-normally distributed. These findings were explained by Ott (1990) with the hypothesis of successive random dilution events. In the present case a single log-normal function can approximate the distributions only within an average relative deviation of about 40%. As a better approximation the gamma distribution has been suggested because it might fit the wings of the PDF better than a log-normal function (Comtois, 2000). Whereas the overall quality of fit could be improved with this function, the approximation of the central part of the PDF is quite unsatisfactory. The superposition of two log-normal functions according to eq. (1), on the other hand, fits both the sharp central peak and the broad wings of the PDF with average relative deviations between fit and PDF of less than 20% over four orders of magnitude in particle number concentration. It remains to be shown if this mathematical description implies a second underlying process controlling aerosol variability. Each of the log-normal functions in eq. (1) has the parameters total frequency of occurrence $F_{t,i}$ and geometric standard deviation σ_i, the third parameter being $\ln 1 = 0$ after normalization of the frequencies of occurrence with their median values:

$$f(n) = \sum_{i=1}^{2} F_{t,i} \exp\left(-\frac{(\ln n)^2}{2(\ln \sigma_i)^2}\right). \quad (1)$$

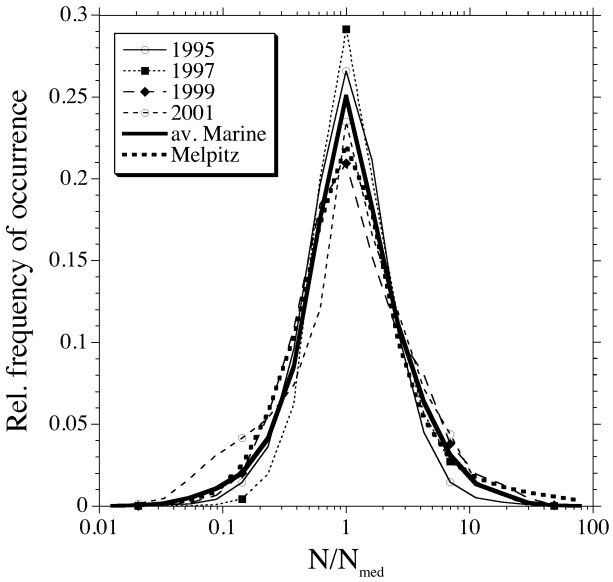

Fig 5. Variability of size-averaged and median-normalized number concentrations in the uncontaminated marine boundary layer, given as relative frequencies of occurrence during the four marine aerosol experiments listed in Table 1 and as an average over all marine data (thick black line). For comparison the corresponding average variability of the continental data from Melpitz, Germany is shown as a thick dashed line.

Table 3. Parameters of the 2-log-normal fit of the average size and concentration normalized probability density function of submicrometre number concentrations of the marine aerosol and at the continental site Melpitz (*cf.* Table 1 for details of the experiments): $F_{t,i}$, total frequency of occurrence of mode i; σ_i. geometric standard deviation of mode i

Aerosol	$F_{t,1}$	σ_1	$F_{t,2}$	σ_2
Marine	0.16	2.7	0.090	1.4
Melpitz	0.13	3.0	0.091	1.7

The four parameters of the two log-normal fits for the average marine PDF and for the Melpitz size distributions are listed in Table 3.

4.3. Persistence of the marine number size distribution

With simple coagulation dynamics of the median size distributions of the five data sets, rough estimates of size-dependent coagulation particle lifetimes can be derived. These lifetimes were calculated from the inverse of the coagulation loss rates of a given particle size against the respective median size distributions. The loss rates are strongly controlled by the weight of the accumulation mode in the overall size distribution (Walter, 1973). Consequently, because of rather similar accumulation modes (*cf.* Table 2), similar coagulation lifetimes are calculated for the experiments in 1995, 1999 and 2001. They increase monotonically from about 10 h at 3 nm particle diameter to about 5000 h at 100 nm. A lifetime corresponding to the maximum length of 120 h in back trajectories is reached in these three experiments for particles of about 10 nm diameter. Because of a factor of two more accumulation mode particles over the North Atlantic (ACE-2) the respective coagulation lifetimes are shortened by a factor of four and they are shifted to smaller values by another factor of three at the continental site as compared with ACE-2.

With autocorrelation the persistence of the marine submicrometre particle size distribution was investigated statistically. This type of analysis has been used for surface data of urban size distributions (Wehner and Wiedensohler, 2002), with the integral aerosol properties of scattering coefficient and optical depth by Charlson (2000) and Anderson et al. (2003), and with aircraft measurements of particle number concentrations by Hermann et al. (2003). Long unbroken high-resolution time-series are required for autocorrelations. Of the four marine aerosol experiments only the Cape Grim dataset was suitable for this purpose. All other data were taken either on moving ships and/or in conditions of rapidly varying air mass, which caused many interruptions due to the set condition of $\geq$120 h traveltime from the nearest land.

In Fig. 6a autocorrelation coefficients for the number concentrations of the Cape Grim time-series are shown for lag times between zero and 60 h. The coefficients are shown at five particle size ranges with different temporal evolution. Additionally, autocorrelation coefficients were calculated for the total number concentrations. Consistent with the simple coagulation dynamics, autocorrelations strongly increase from the smallest to the larges size, indicating that the few occurrences of UFP are based on very local short-term incidences whereas Aitken mode particles are highly persistent in the MBL and accumulation mode particles even more so. The same holds for the total number concentration, because it is dominated by the persistent Aitken particles. No diurnal variations are visible in the present marine data set.

This rather persistent marine aerosol is contrasted with corresponding continental results derived by the corresponding autocorrelation analysis of the Melpitz data, the results of which are given in Fig. 6b. As expected from coagulation dynamics, autocorrelation coefficients for particle diameters below 100 nm are much lower at the continental station than at Cape Grim. For larger particles their autocorrelation at the continental site is comparable to marine conditions. The drop-off of autocorrelation coefficients with lag time at the UFP sizes is not quite as rapid as over the ocean, and diurnal variations are visible at all particle sizes. The strongly size-dependent amplitudes of the diurnal maxima in the autocorrelation coefficients clearly indicate that they are not just controlled by diurnal dilution processes in the continental boundary layer. The insolation-controlled photochemical processes strongly affect gas-to-particle formation of small particles.

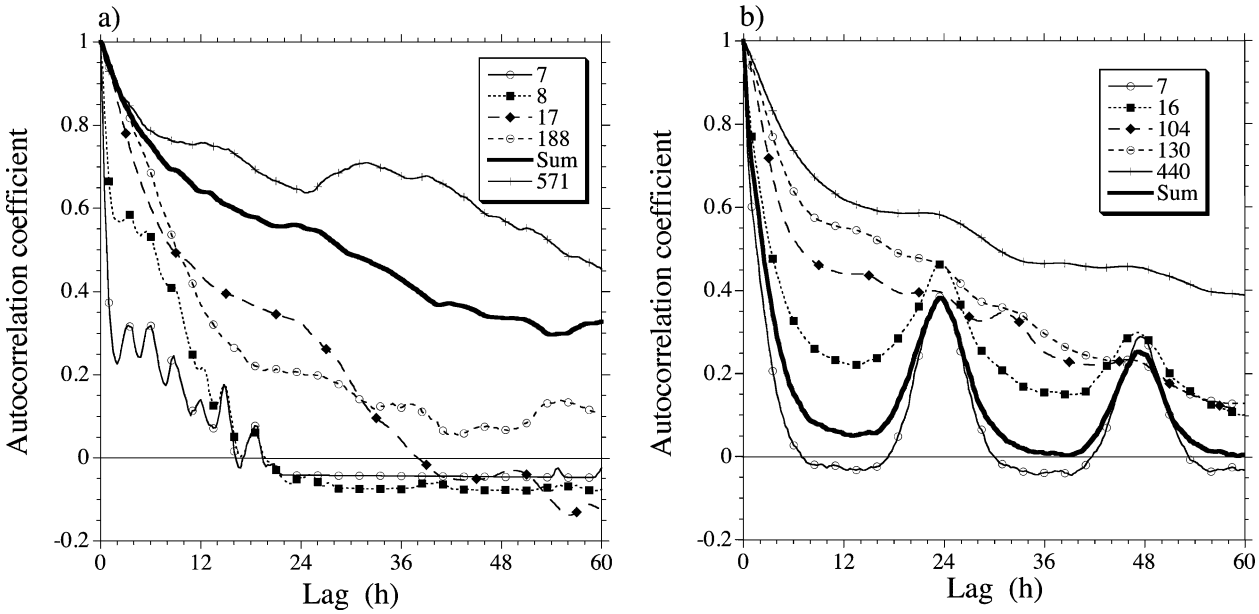

Fig 6. (a) Autocorrelation coefficients of number concentrations at 7 (open diamonds), 8 (full squares), 17 (full diamonds), 188 (open circles) and 571 nm (crosses) particle diameter and total concentration (thick line) for time lags between 0 and 60 h at Cape Grim, Tasmania; (b) As (a) but at Melpitz, Germany and particle diameters 7 (open diamonds), 16 (full squares), 104 (full diamonds), 130 (open circles) and 440 nm (crosses), and total concentrations (thick line) (see Table 1 for details of the experiment).

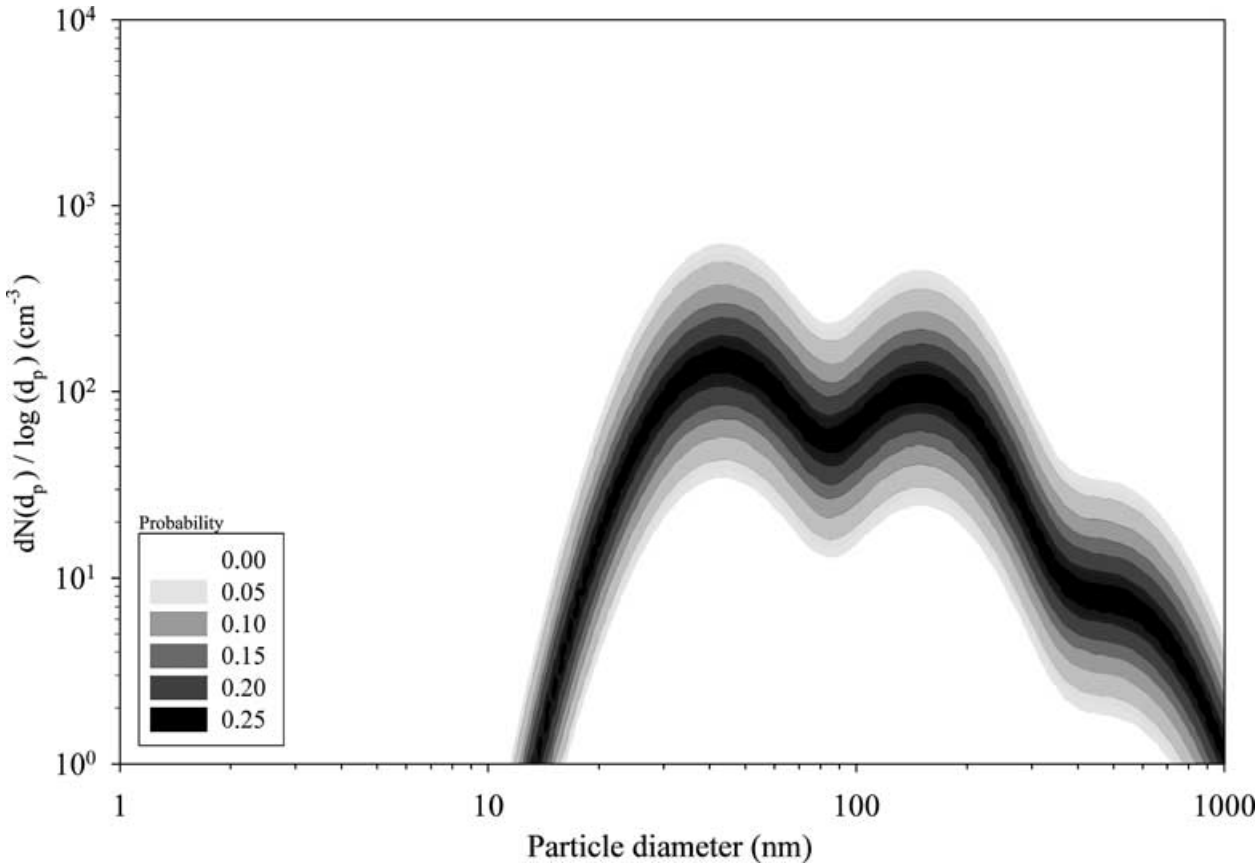

Fig 7. Median log-normal approximation of the four-modal submicrometre marine number size distributions averaged over the four experiments listed in Table 1. Probabilities of number concentrations about the median distributions are given according to the model of eq. (1) for the range 0.1 to 10 times the median concentrations.

When calculating a size-dependent lag time by which autocorrelation coefficients drop of to a given level, e.g. 0.5, a modal structure appears in the marine aerosol (*cf.* Fig. 2), which shows maxima in lag time near the most frequent geometric mean diameters. The upper end of the analysed size range exhibits lag times above 100 h at Cape Grim, which lies in the Southern Hemisphere belt with high westerly wind speeds generating persistently large numbers of sea-salt particles. In the continental aerosol only weak maxima in lag time appear below 100 nm particle diameter. Beyond that size, a broad shoulder with lag times >20 h appears in the continental aerosol, which can be interpreted as the effect of the large European source region with similar aerosol sources.

5. Conclusions

Submicrometre dry number size distributions from four marine and one continental aerosol experiment were evaluated jointly in the present study. In the marine experiments only data with back trajectories of at least 120 h without land contact were used to minimize continental contamination. Log-normal functions were fitted to the size distributions. Statistics of geometric mean diameters d_{g0} of these fits reveal maxima in their frequency of occurrence, with which four modes can be delineated.

Basic statistics of the non-aggregated size-dependent particle number concentrations ($PDF_N(d_p)$) of the marine aerosol indicate a closed character of the size distribution at the lower size limit as opposed to the open character of corresponding continental data. Together with the infrequent occurrences of marine particles below 20 nm this finding supports hypotheses and model results suggesting low probabilities of homogeneous nucleation in the MBL. $PDF_N(d_p)$ exhibits relative maxima or modes as well as d_{g0}. If the variability of the size distribution were only caused by random dilutions of the whole submicrometre particle population then one would expect these modes to coincide with the log-normal modes, and they roughly do above the UFP size range.

From the statistics of $PDF_N(d_p)$ the variability of submicrometre marine number concentrations could be parametrized with a bimodal log-normal function that quantifies the probability of finding different number concentrations about a given median value. Together with a four-modal log-normal approximation of the submicrometre marine size distribution itself, this model allows a statistical representation of the marine aerosol that facilitates comparisons of experiments and validation of aerosol models. Figure 7 synthesizes the present data set from the four marine experiments according to this model approach. It can be seen as a statistical synthesis of the corresponding primary data shown in Fig. 4, which comprises analytical expressions of the distribution and its statistics as well. Using size-independent concentration statistics in Fig. 7 is a compromise that reflects the limited particle-counting statistics of the present instrumentation at both ends of the submicrometre size range. In the UFP size range fast mixing type CPCs should improve statistics (e.g. Wang et al., 2002). At the other end of the size range optical particle counters or high-flow DMAs (e.g. Kreisberg et al., 2001; Leinert, 2002) would improve statistics.

Detailed aerosol dynamics models of the marine atmosphere will be needed to elucidate the whole range of variability as demonstrated with the present study. The validity of such models can be tested with the analytical functions, which were fitted to the frequencies of occurrence of median-normalized particle number concentrations as derived from the present evaluation.

Persistence of the marine aerosol was the other major subject of the study. As expected qualitatively from coagulation lifetime considerations, autocorrelation at the one fixed marine site with a minimum of interruptions in time-series revealed a strong size dependency of persistence in particle number concentrations, with shortest persistence at the smallest sizes. Interestingly, in the marine aerosol (at Cape Grim) persistence exhibits a size dependency that largely matches the modes in d_{g0}, i.e. near the most frequent geometric mean diameters number concentrations are most persistent. Over the continent persistence of particle numbers is strongly constrained by diurnal meteorological processes and aerosol dynamics. Thus, no strong modal structure appears in the size-dependent persistence at Melpitz. As with the aerosol variability, marine aerosol processes in aerosol dynamics models can be tested with these findings.

6. Acknowledgments

Dave Covert, Andy Maßling, and Diana Weise contributed to the collection of size distributions during the four marine experiments. Diane Galgon kindly calculated and classified the back trajectories for 1995 and 1997. Olaf Hellmuth's comments on the value of statistical aerosol information are highly appreciated.

References

Anderson, T., Charlson, R., Winker, D., Ogren, J. and Holmen, K. 2003. Mesoscale variations of tropospheric aerosols. *J. Atmos. Sci.* **60**, 119–136.

Bates, T. S., Coffman, D. J., Covert, D. S. and Quinn, P. K. 2002. Regional marine boundary layer aerosol size distributions in the Indian, Atlantic, and Pacific Oceans: a comparison of INDOEX measurements with ACE-1, ACE-2, and Aerosols99. *J. Geophys. Res.* **107**(D19), doi:10.1029/2001/JD001174.

Bates, T. S., Huebert, B. J., Gras, J. L., Griffiths, F. B. and Durkee, P. A. 1998a. International Global Atmospheric Chemistry (IGAC) project's first aerosol experiment (ACE 1): overview. *J. Geophys. Res.* **103**(D13), 16 297–16 318.

Bates, T. S., Kapustin, V. N., Quinn, P. K., Covert, D. S., Coffman, D. J. et al. 1998b. Processes controlling the distribution of aerosol particles in the lower marine boundary layer during the first Aerosol Characterization Experiment (ACE 1). *J. Geophys. Res.* **103**(D13), 16 369–16 383.

Bates, T. S., Quinn, P. K., Covert, D. S., Coffman, D. J., Johnson, J. E. et al. 2000. Aerosol physical properties and processes in the lower

marine boundary layer: a comparison of shipboard sub-micron data from ACE-1 and ACE-2. *Tellus* **52B**, 258–272.

Benkovitz, C. M., Berkowitz, C. M., Easter, R. C., Nemesure, S., Wagener, R. et al. 1994. Sulfate over the North Atlantic and adjacent continental regions: evaluation for October and November, 1986 using a three-dimensional model driven by observation-derived meteorology. *J. Geophys. Res.* **99**(D10), 20 725–20 756.

Benkovitz, C. M. and Schwartz, S. E. 1997. Evaluation of modeled sulfate and SO_2 over North America and Europe for four seasonal months in 1986–1987. *J. Geophys. Res.* **102**(D21), 25 305–25 338.

Birmili, W. 2001. A moment-preserving parameterization of wide particle size distributions. *J. Aerosol Sci.* **32**, S191–S192.

Birmili, W. and Wiedensohler, A. 1997. The design of a twin-differential mobility particle sizer for a wide size range and great operational stability. *J. Aerosol Sci.* **28**(S1), S145–S146.

Birmili, W. and Wiedensohler, A. 2000. New particle formation in the continental boundary layer: meteorological and gas phase parameter influence. *Geophys. Res. Lett.* **27**(20), 3325–3328.

Birmili, W., Wiedensohler, A., Heintzenberg, J. and Lehmann, K. 2001. Atmospheric particle number size distribution in Central Europe: statistical relations to air masses and meteorology. *J. Geophys. Res.* **106**(D23), 32 005–32 018.

Charlson, R. J. 2000. Extending atmospheric aerosol measurements to the global scale. In: *Topics in Atmospheric and Interstellar Physics and Chemistry* (ed.C. Boutron). Les Éditions de Physique, Les Ulis, France, pp. 67–81.

Clarke, A. D., Li, Z. and Litchy, M. 1996. Aerosol dynamics in the equatorial Pacific Marine boundary layer: microphysics, diurnal cycles and entrainment. *Geophys. Res. Lett.* **23**(7), 733–736.

Comtois, P. 2000. The gamma distribution as the true aerobiological probability density function (PDF). *Aerobiologica* **16**(2), 171–176.

Covert, D. S., Gras, J. L., Wiedensohler, A. and Stratmann, F. 1998. Comparison of directly measured CCN with CCN modeled from the number-size distribution in the marine boundary layer during ACE 1 at Cape Grim, Tasmania. *J. Geophys. Res.* **103**(D13), 16 597–16 608.

Covert, D. S., Wiedensohler, A., Aalto, P., Heintzenberg, J., McMurry, P. H. et al. 1996. Aerosol number size distributions from 3 to 500 nm diameter in the arctic marine boundary layer during summer and autumn. *Tellus* **48B**, 197–212.

Heintzenberg, J., Covert, D. S. and Van Dingenen, R. 2000. Size distribution and chemical composition of marine aerosols: a compilation and review. *Tellus* **52B**(4), 1104–1122.

Hermann, M., Heintzenberg, J., Wiedensohler, A., Brenninkmeijer, C. A. M., Heinrich, G. et al. 2003. Meridional distributions of aerosol particle number concentrations in the upper troposphere and lower stratosphere obtained by CARIBIC flights. *J. Geophys. Res.* **108**(D3), doi:10.1029/2001JD0010077.

Jacobson, M. Z. 2001. Global direct radiative forcing due to multicomponent anthropogenic and natural aerosols. *J. Geophys. Res.* **106**(D2), 1551–1568.

Kreisberg, N. M., Stolzenburg, M. R., Hering, S. V., Dick, W. D. and McMurry, P. H. 2001. A new method for measuring the dependence of particle size distribution on relative humidity, with application to the Southeastern Aerosol and Visibility Study. *J. Geophys. Res.* **106**(D14), 14 935–14 950.

Kulmala, M., Vehkamäkia, H., Petäjä, T., Maso, M. D., Lauri, A. et al. 2004. Formation and growth rates of ultrafine atmospheric particles: a review of observations. *J. Aerosol Sci.* **35**, 143–176.

Langner, J., Bates, T. S., Charlson, R. J., Clarke, A. D., Durkee, P. A. et al. 1993. The global atmospheric sulfur cycle: an evaluation of model predictions and observations. Report CM-81, Stockholm University.

Leck, C. and Bigg, E. K. 1999. Aerosol production over remote marine areas—a new route. *Geophys. Res. Lett.* **23**, 3577–3581.

Leinert, S. 2002. *Hygroscopicity of Micrometer-sized Aerosol Particles—a New Measurement Technique*. PhD Thesis, University of Leipzig.

Mäkelä, J. M., Koponen, I. K., Aalto, P. and Kulmala, M. 2000. One-year data of submicron size modes of tropospheric background aerosol in southern Finland. *J. Aerosol Sci.* **31**(5), 595–611.

Ott, W. R. 1990. A physical explanation of the lognormality of pollutant concentrations. *J. Air Waste Manage. Assoc.* **40**, 1378–1383.

Raes, F. 1995. Entrainment of free tropospheric aerosols as a regulating mechanism for cloud condensation nuclei in the remote marine boundary layer. *J. Geophys. Res.* **100**(D2), 2893–2903.

Raes, F., Bates, T., Vogelenzang, D., van Liedekerke, M. and Verver, G. 2000. The second aerosol characterization experiment (ACE-2): general overview and main results. *Tellus* **52B**(2), 111–125.

Rasch, P. J., Barth, M. C. and Kiehl, J. T. 2000. A description of the global sulfur cycle and its controlling processes in the NCAR CCM3. *J. Geophys. Res.* **105**(D1), 1367–1385.

Russell, P. B. and Heintzenberg, J. 2000. An overview of the ACE 2 Clear Sky Column Closure experiment (CLEARCOLUMN). *Tellus* **52B**, 463–483.

Shaw, G. E., Benner, R. L., Cantrell, W. and Clarke, A. D. 1998. On the regulation of climate: a sulfate particle feedback loop involving deep convection. *Clim. Change* **39**, 23–33.

Tully, M. and Downey, A. 2003. *Back Trajectories to Cape Grim: Investigating Sources of Error*, Baseline 1999–2000, Bureau of Meteorology and CSIRO Atmospheric Research, Melbourne, pp. 8–12.

Tunved, P., Hansson, H.-C., Kulmala, M., Aalto, P., Viisanen, Y. et al. 2003. One year boundary layer aerosol size distribution data from five Nordic background stations. *Atmos. Chem. Phys.* **3**, 2183–2205.

Walter, H. 1973. Coagulation and size distribution of condensation aerosols. *J. Aerosol Sci.* **4**, 1–15.

Wang, J., McNeill, V. F., Collins, D. R. and Flagan, R. C. 2002. Fast mixing condensation nucleus counter: application to rapid scanning differential mobility analyzer measurements. *Aerosol Sci. Technol.* **36**(6), 678–689.

Wehner, B. and Wiedensohler, A. 2002. Long term measurements of submicrometer urban aerosols: statistical analysis for correlations with meteorological conditions and trace gases. *Atmos. Chem. Phys.* **3**, 867–879.

Wilson, J., Cuvelier, C. and Raes, F. 2001. A modeling study of global mixed aerosol fields. *J. Geophys. Res.* **106**, 34 081–34 108.